

# Ultrasensitive Gas Sensors Based on Electrospun TiO<sub>2</sub> and ZnO †

Ambra Fioravanti <sup>1</sup>, Sara Morandi <sup>2</sup>, Alberto Rubin Pedrazzo <sup>2</sup>, Pierangiola Bracco <sup>2</sup>, Marco Zanetti <sup>2</sup>, Maela Manzoli <sup>3</sup>, Mauro Mazzocchi <sup>4</sup> and Maria Cristina Carotta <sup>1,\*</sup>

<sup>1</sup> Laboratorio Sensori e Nanomateriali, C.N.R.-IMAMOTER, 44124 Ferrara, Italy; a.fioravanti@imamoter.cnr.it

<sup>2</sup> Dipartimento di Chimica and NIS Inter-departmental Center, Università di Torino, 10124 Torino, Italy; sara.morandi@unito.it (S.M.); alberto.rubinpdrizzo@unito.it (A.R.P.); pierangiola.bracco@unito.it (P.B.); marco.zanetti@unito.it (M.Z.)

<sup>3</sup> Dipartimento di Scienza e Tecnologia del Farmaco, Università di Torino, 10124 Torino, Italy; maela.manzoli@unito.it

<sup>4</sup> C.N.R.-ISTEC, 10135 Faenza, Italy; mauro.mazzocchi@istec.cnr.it

\* Correspondence: mc.carotta@imamoter.cnr.it; Tel.: +39-053-273-5668

† Presented at the Eurosensors 2017 Conference, Paris, France, 3–6 September 2017.

Published: 5 September 2017

**Abstract:** New sensors for detecting gases at low concentration were successfully developed. Two metal oxide materials, zinc oxide and titanium dioxide, usually employed both in gas sensing as well as in photocatalytic application, were synthesized both through a traditional sol-gel method and an electrospinning technique. The corresponding thick films were considered with respect to the target gases (acetone for ZnO and carbon monoxide for TiO<sub>2</sub>) for comparing their functional properties.

**Keywords:** metal oxides gas sensors; nanomaterials; electrospinning technique; sol-gel method

## 1. Introduction

The demand of real time, low cost and small size sensors is continuously increasing to control a large variety of parameters such as environmental, food quality, biomedical, etc. In the context of gas sensors, great advantages have been achieved through an extensive investigation on the semiconductor metal oxides (MOX) benefiting from progresses in nano-technology, recently occurred. In particular, the detection at very low concentration of gases is of paramount importance for medical and environmental applications to detect gases such as acetone, ethanol, isoprene and benzene.

The aim of this work is to develop nanomaterials for high sensitivity gas sensors. TiO<sub>2</sub> and ZnO have been selected because they have been widely investigated in solar cells, photocatalysts and gas sensors [1]. TiO<sub>2</sub> and ZnO can be obtained in form of nanostructures via physical or chemical processes in different morphologies. Among these techniques, electrospinning and sol-gel methods have been adopted to compare their morphological, structural, optical and functional properties.

Electrospinning represents a new, simple and versatile method for generating ceramic porous nanofibers with interconnective pores and high specific surface area [2]. The sol-gel synthesis is a traditional method to prepare nanopowders with tailored properties, in terms of purity, morphology and grain size homogeneity.

The thick films produced from the synthesized nanopowders have been measured through dynamical responses in presence of the target gases. Moreover, Arrhenius plots and energy barriers versus temperature in dry air as well as FTIR analysis (performed onto ZnO materials during

interaction with acetone at the same working temperatures of the sensors) have been carried out in order to investigate on the Schottky barrier model and on the electronic properties of the investigated materials.

## 2. Materials and Methods

Solutions for electrospinning were prepared by mixing: (i) ethanol (55.6 wt %), PVP (9.5 wt %), acetic acid (23.6 wt %) and Ti (IV) butoxide (11.2 wt %); (ii) ethanol (28 wt %), PVP (16 wt %), water (25 wt %) and zinc nitrate (32 wt %). For both Ti and Zn precursor solutions, the electrospinning process was performed in air, at RT with a feeding rate of 10  $\mu\text{L}/\text{min}$ , a voltage of 30 kV and a working distance of 14 cm. The generated fibers underwent calcination at 450  $^{\circ}\text{C}$  obtaining  $\text{TiO}_2$  and ZnO (here named ES). Starting from the same precursors, ZnO and  $\text{TiO}_2$  were synthesized through a sol-gel route (here named SG). Ti (IV) n-butoxide was dissolved in absolute ethanol (0.23 M) and added to a solution of ethanol/water 1:1 vol. For ZnO, a proper amount of ammonium hydroxide was added to a water solution 0.05 M of  $\text{Zn}(\text{NO}_3)_2 \cdot 6\text{H}_2\text{O}$  to reach a pH of 10 and ageing the solution at RT for 1 h. The precipitates,  $(\text{Ti}(\text{OH})_4)$  and  $\epsilon\text{-Zn}(\text{OH})_2$ , were filtered, washed, dried and finally calcined at 400 and 450  $^{\circ}\text{C}$  in air for 2 h, respectively obtaining anatase  $\text{TiO}_2$  and ZnO.

The sensing films were deposited through screen-printing technique onto miniaturized alumina substrates each one provided with a heater element and interdigitated contacts, firing all samples at 650  $^{\circ}\text{C}$ . Hereinafter, the  $\text{TiO}_2$  films will be named TES, if obtained by electrospinning, and TSG by sol-gel; the same for ZnO films, ZES and ZSG, respectively.

X-ray diffraction (XRD) patterns of the samples were collected to determine the crystalline phases and the average crystallite sizes by applying the Scherrer's formula on the (101) diffraction peak. The specific surface areas were determined through the Brunauer-Emmett-Teller (BET) method to the adsorption/desorption isotherms of  $\text{N}_2$  at 77 K. Morphological characterization of the samples was performed by Field Emission Scanning Electron Microscopy (FE-SEM).

Absorption IR spectra were run on the powder samples compressed in self-supporting discs and placed in a commercial heated stainless steel cell allowing thermal treatments in situ under vacuum or controlled atmosphere. The IR spectra were recorded for ZnO during the interaction with a mixture acetone/ $\text{O}_2$  (1:5,  $p_{\text{acetone}} = 5$  mbar) at increasing temperature up to 400  $^{\circ}\text{C}$ .

The flow-through technique was used to test the electrical properties of the sensors, at a flow rate of 0.5 L/min using synthetic air as carrier gas. Conductance as a function of temperature (300–900 K) and surface barrier height (carried out using the method of temperature-stimulated conductance measurements) were measured to determine the intergranular energy barrier versus temperature. Moreover, dynamic responses of sensing films were obtained in presence of mixture of different gases varying the operating temperature from 350 to 550  $^{\circ}\text{C}$ , defining the sensor response as ratio between the conductance in presence of the target gas and the conductance in air.

## 3. Results and Discussion

XRD analysis showed a hexagonal wurtzite structure for ES and SG-ZnO and anatase phase for ES and SG- $\text{TiO}_2$  calcined at 450  $^{\circ}\text{C}$ . Both anatase and rutile phase are present calcining at 650  $^{\circ}\text{C}$  (Figure 1).

For both ZnO and  $\text{TiO}_2$ , average crystallite size of the material obtained via electrospinning is comparable to that of the material obtained via sol-gel. This is not reflected on the specific surface areas (see Table 1). In particular, SG materials show surface areas higher than the corresponding ES materials. This is related to the presence of meso-pores in the SG samples, which volumes are 0.0986  $\text{cm}^3/\text{g}$  and 0.2922  $\text{cm}^3/\text{g}$  for SG-ZnO and SG- $\text{TiO}_2$ , respectively. The mesoporosity is particularly marked for SG- $\text{TiO}_2$  and this justifies the surface area markedly higher with respect to ES- $\text{TiO}_2$ .

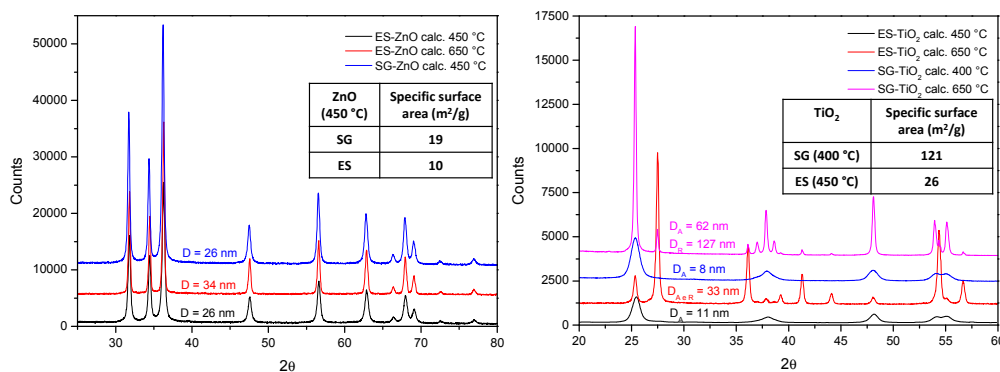


**Figure 1.** X-ray diffraction patterns for all synthesized powders; in the insets the specific surface areas.

In Figure 2, the SEM images reveal that the ES-TiO<sub>2</sub> sample retains, after the thermal treatment, the fibrous nature characteristic of the as-electrospun material. The fibers are not single crystals but are particle aggregates. SG-TiO<sub>2</sub> are constituted by globular particle aggregates observable also for the ZnO samples; the particles of ES-ZnO are smaller than that of SG-ZnO. It is worth of note that ES-ZnO does not retain the fibrous morphology shown by ES-TiO<sub>2</sub>.

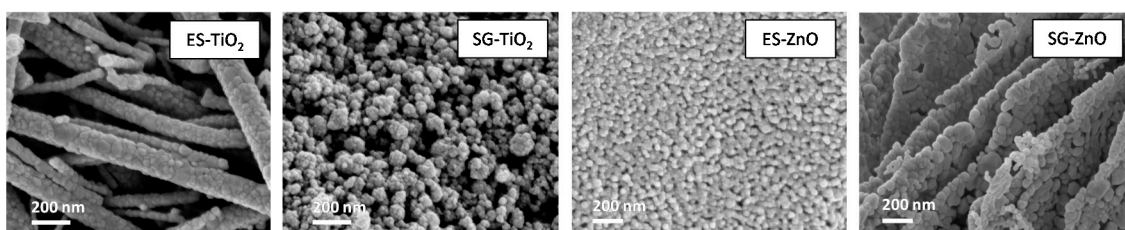


**Figure 2.** SEM micrographs of the ES and SG-TiO<sub>2</sub> films fired at 650 °C and of ES- and SG-ZnO powders calcined at 450 °C.

IR absorption spectra of ZnO materials in interaction with a mixture acetone/O<sub>2</sub> at increasing temperature are reported in Figure 3. The spectra of both ZnO samples are characterized by the increase of the electronic absorption related to the transition of electrons from mono-ionized oxygen vacancies to the conduction band up to 350 °C. At 400 °C the electronic absorption band decreases due to partial re-oxidation of the surface caused by oxygen in the mixture. The bands of the gaseous acetone are superimposed to the broad electronic band and decrease in intensity on increasing temperature, being acetone consumed by the surface reactions. Surface carbonates (bands at 1440 and 1550 cm<sup>-1</sup>) are formed by the chemisorption of CO<sub>2</sub> due to the acetone oxidation. The integrated intensity of the electronic absorption exhibits higher value for the ES-ZnO than for SG-ZnO, in agreement with electrical measurements that reveal higher response to acetone for ES than for SG sample.

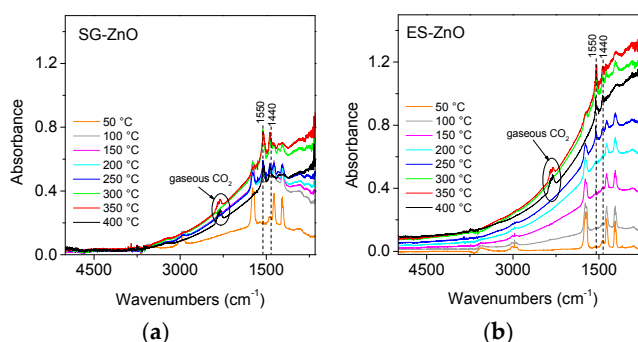


**Figure 3.** FT-IR spectra of SG-ZnO (a) and ES-ZnO (b) upon acetone/O<sub>2</sub> interaction at increasing temperature up to 400 °C.

Concerning the gas sensing properties, at first, all ZnO films have been tested toward acetone, acetaldehyde, isoprene, ethanol and ammonia (10 ppm in dry air).

Dynamic responses were achieved with the operating temperature ranging from 350 to 550 °C. It resulted that all investigated samples exhibited the best performances towards acetone, giving the other gases weak interference with respect to it, except isoprene and ethanol for which the response was about one third with respect to acetone. In Figure 4, a series of responses to 1 ppm of acetone in dry air at the working temperature of 400 °C for ZES samples and 450 °C for ZSG ones are reported. ZES samples show the best performance with respect to ZSG ones. This fact is expected due to the smaller grain size of ES-ZnO material and confirmed by IR analysis. Moreover, measurements of intergranular energy barrier versus temperature (not shown here), exhibited a greater difference between the minimum and the maximum of the barrier, being 1.1 eV for ZES samples and 0.6 for ZSG ones. It means that in ZES samples many more ionosorbed oxygens than in ZSG are available for surface chemical reactions causing a greater response to gases. Moreover, other measurements (not reported here) showed the ability of this material to detect acetone at concentrations low down to tens of ppb.

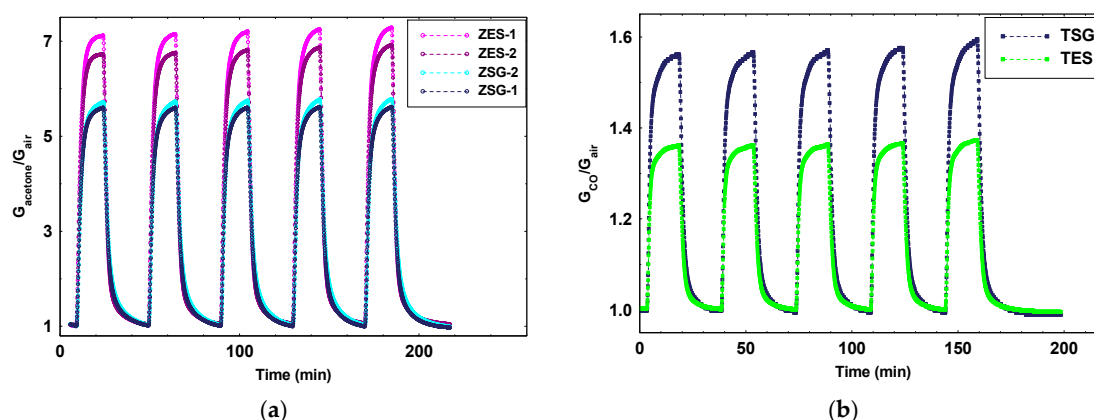


**Figure 4.** Dynamic responses to 1 ppm of acetone for ZES and ZSG sensors reported as  $G_{\text{acetone}}/G_{\text{air}}$  (a) and 2 ppm of carbon monoxide for TSG and TES sensors reported as  $G_{\text{CO}}/G_{\text{air}}$  (b).

Passing to TiO<sub>2</sub> films, they were tested toward carbon monoxide (10–1 ppm), benzene (2 ppm), hydrogen sulfide (5 ppm) and sulphur dioxide (5 ppm). Both synthesized materials have been able to detect all the tested gases. In particular, they resulted able to detect carbon monoxide at concentrations suitable for the environmental application. However, differently from the case of ZnO, SG-TiO<sub>2</sub> exhibited the best performances toward each tested gas, despite the very fine particles of which the fibers of the electrospun TiO<sub>2</sub> are constituted. The lower ability of ES-TiO<sub>2</sub> to detect very low concentration of gases could be ascribed to: (i) a great percentage of rutile phase present on the films fired at 650 °C; (ii) the elongated structure could not guarantee an adequate number of contacts between fibers to favor the formation of Schottky barriers. However, further investigations must be carried out to verify these points.

**Conflicts of Interest:** The authors declare no conflict of interest.

## References

1. Sun, R.-D.; Nakajima, A.; Fujishima, A.; Watanabe, T.; Hashimoto, K. Photoinduced Surface Wettability Conversion of ZnO and TiO<sub>2</sub> Thin Films. *J. Phys. Chem. B* **2001**, *105*, 1984–1990.
2. Choi, S.K.; Kim, S.; Lim, S.K.; Park, H. Photocatalytic Comparison of TiO<sub>2</sub> Nanoparticles and Electrospun TiO<sub>2</sub> Nanofibers: Effects of Mesoporosity and Interparticle Charge Transfer. *J. Phys. Chem. C* **2010**, *114*, 16475–16480.

3. Chiorino, A.; Ghiotti, G.; Prinetto, F.; Carotta, M.C.; Malagu, C.; Martinelli, G. Preparation and Characterization of SnO<sub>2</sub> and WO<sub>x</sub>-SnO<sub>2</sub> Nanosized Powders and Thick Films for Gas Sensing. *Sens. Actuators B Chem.* **2001**, *78*, 89–97.



© 2017 by the authors. Licensee MDPI, Basel, Switzerland. This article is an open access article distributed under the terms and conditions of the Creative Commons Attribution (CC BY) license (<http://creativecommons.org/licenses/by/4.0/>).